11-2010

Photoinduced Charge Separation In Platinum Acetylide Oligomers

Chen Liao

James E. Yarnell

Ksenija D. Glusac
Bowling Green State University, kglusac@bgsu.edu

Kirk S. Schanze

Photoinduced Charge Separation in Platinum Acetylide Oligomers†

Chen Liao,‡ James E. Yarnell,§ Ksenija D. Glusac,§ and Kirk S. Schanze*,‡

Department of Chemistry, University of Florida, P.O. Box 117200, Gainesville, Florida 32611, and Department of Chemistry, Bowling Green State University, Bowling Green, Ohio 43403

Received: April 19, 2010; Revised Manuscript Received: June 11, 2010

The series of three donor-spacer-acceptor complexes, **DPAF-Ptn-NDI**, has been synthesized and characterized using time-resolved absorption spectroscopy. In these complexes, the donor is a (diphenylamino)-2,7-fluorenylene (DPAF) unit, the acceptor is a naphthalene diimide (NDI), and the spacers are a series of platinum acetylides of varying lengths, $[-Pt(PBu_3)_2-C\equiv C-Ph-C\equiv C-]_n$ (where Bu = *n*-butyl, Ph = 1,4-phenylene and $n = 1$, 2, and 3). Electrochemistry indicates that the **DPAF-Ptn-NDI** system has a charge transfer state at ca. 1.5 eV above the ground state that is based on one electron transfer from the DPAF donor to the NDI acceptor. Transient absorption spectroscopy on time scales ranging from 0.2 ps to 1 μs reveals that excitation of all of the complexes leads to production of the charge transfer state with nearly unit quantum efficiency. The rates for charge separation and charge recombination are not strongly dependent upon the length of the platinum acetylide spacer, suggesting that the spacer is actively involved in the electron (hole) transport processes. Analysis of the experimental results leads to a model in which charge separation and charge recombination occur by hole-hopping via states localized on the $[-Pt(PBu_3)_2-C\equiv C-Ph-C\equiv C-]_n$ bridge.

Introduction

Photoinduced electron transfer (PET) reactions have been studied extensively during the past several decades, and important contributions to this field have been made by many groups.[1,2] The study of PET processes in molecular dyad and triad assemblies has provided important experimental insight regarding the effects of free energy on rate (Marcus theory and the inverted region), solvent, molecular geometry, and spacer effects on donor−acceptor electronic coupling. Many significant contributions in the area of PET in dyad and triad assemblies have come from the Wasielewski group.[3−5] Most early work in the area of dyads and triads sought to mimic the early steps involved in photosynthesis, including charge separation and charge storage.[6−8] However, more recent studies have explored π-conjugated donor−acceptor assemblies as "molecular electronic devices", which may be capable of carrying out basic tasks of a molecular optoelectronic device such as carrier transport (wire) or switching (transistor).[9−18] These latter studies often utilize molecular assemblies in which the spacer consists of a rigid π-conjugated electronic system that provides robust donor−acceptor separation but maintains a strong degree of electronic coupling between the moieties.

We have an ongoing interest in the study of polymers and oligomers that feature the platinum acetylide as the basic repeat unit, e.g., $[-Pt(PR_3)_2-C\equiv C-Ar-C\equiv C-]$, where Ar = an arylene such as 1,4-phenylene or 2,5-thienylene and the geometry at the platinum center is trans.[19−22] The platinum acetylide system is π-conjugated and consequently is photoactive and electroactive. For example, oligomers or polymers of the type $[-Pt(PR_3)_2-C\equiv C-Ph-C\equiv C-]_n$ (Ph = 1,4-phenylene) absorb in the near-UV region and exhibit weak fluorescence and relatively strong phosphorescence at ambient temperature. Spectroscopic studies of platinum acetylide polymers and oligomers show that the singlet excited state is delocalized over more than three repeat units, whereas the triplet state is spatially confined to just over one repeat unit.[19] Studies of the polaron states (cation and anion radicals) show that the charged states are spatially confined, much like the triplet state.[20] Given these results, it can be expected that the platinum acetylide system could serve as a spacer supporting charge separation; however, the existence of energetically accessible hole and electron states may facilitate electron (or hole) transport over relatively long distances.

To explore the properties of the platinum acetylide system to serve as a spacer/molecular wire, herein we report photoinduced electron transfer studies of the series of donor−acceptor "dyads" shown in Chart 1. In these systems a (diphenylamino)-2,7-fluorenylene (DPAF) unit serves as an electron donor, and a naphthalenediimide (NDI) moiety as an electron acceptor. These donor and acceptor units are separated by platinum acetylide spacers containing 1, 2, and 3 $[-Pt(PR_3)_2-C\equiv C-Ph-C\equiv C-]$ repeat units. Transient absorption studies on time scales ranging from 200 fs to 100 ns reveal that efficient photoinduced charge transfer occurs, producing a charge separated state with a hole on the DPAF moiety and electron on the NDI acceptor. The results suggest that charge separation occurs via a stepwise pathway, involving an intermediate state with a hole on the platinum acetylide spacer. The rate of charge recombination varies little with spacer length, suggesting that recombination also occurs stepwise via intermediates involving bridge states.

Experimental Section

Synthesis. The syntheses and spectroscopic characterization of the **DPAF-Ptn-NDI** series are described in detail in the Supporting Information.

Absorption and Photoluminescence Spectroscopy. Steady-state absorption spectra were recorded on a Varian Cary 50 or a Cary 100 dual-beam spectrophotometer. Corrected steady-state emission measurements were performed on a Photon Technology International spectrophotometer (QuantaMaster).

† Part of the "Michael R. Wasielewski Festschrift".

* Author to whom correspondence should be addressed. Tel: 352-392-9133, Fax: 352-392-2395. E-mail: kschanze@chem.ufl.edu.

‡ University of Florida.

§ Bowling Green State University.

10.1021/jp103531y
Published on Web 07/01/2010

CHART 1

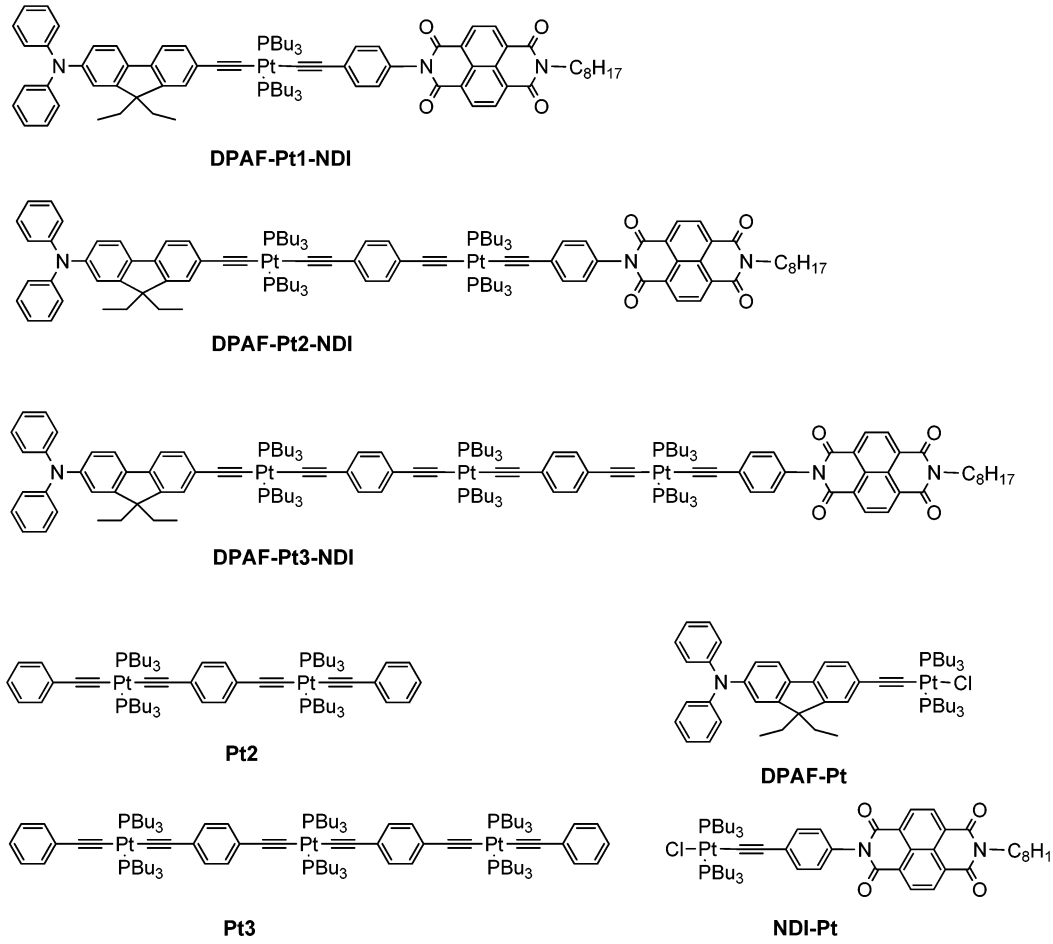

The samples were degassed with argon for 30 min, and optically dilute samples with OD < 0.1 at the excitation wavelength were used. Emission quantum yields were measured using $Ru(bpy)_3Cl_2 \cdot 6H_2O$ as a standard, of which Φ_{fl} was reported to be 0.0379 in aerated water.[23]

Nanosecond Transient Absorption Spectroscopy. Transient absorption (TA) measurements were performed on an in-house apparatus that is described in detail elsewhere.[24] The third harmonic of a Continuum Surelite series Nd:YAG laser (λ = 355 nm, 10 ns fwhm, 5 mJ pulse^{-1}) was used as the excitation source. Probe light was produced by a xenon flash lamp and the transient absorption signal was detected with a gated-intensified CCD mounted on a 0.18 M spectrograph (Princeton PiMax/Acton Pro 180). Sample concentrations were adjusted to approximately 0.6−0.8 absorbance at 355 nm and were degassed with argon for 30 min. A flow cell holding a volume of 10 mL was used and was continuously circulated at the pump−probe region during the measurements. Two-photon excitation TA spectra were recorded on the same system; however, the near-infrared excitation was produced by an OPO (Surelite OPO plus) that was pumped by the 355 nm output of the Continuum Surelite laser. The output of the OPO (λ = 618 nm) was passed through a telescope providing a final beam diameter of 0.7 cm. This beam was focused with a 10 cm focal length lens (Newport Optics), and the sample was positioned at the focal plane of the lens. The sample was contained in a 5 mm i.d. round borosilicate tube.

Picosecond Pump−Probe Spectroscopy. The laser system for the ultrafast transient absorption measurements was described previously.[25] Briefly, the 800 nm laser pulses were produced at a 1 kHz repetition rate by a mode-locked Ti:sapphire laser (Hurricane, Spectra-Physics). The pulse width was determined to be fwhm = 110 fs using an autocorrelator (Positive Light). The output from a Hurricane was split into pump (85%) and probe (8%) beams. The pump beam (800 nm) was sent into a second harmonic generator (Super Tripler, CSK) to obtain a 400 nm excitation source. The energy of the pump beam was ~5 μJ/pulse. The probe beam (800 nm) was delayed by a delay stage (MM 4000, Newport) and then focused into a sapphire crystal for white light continuum generation between 450 and 900 nm. The probe beam in the 350−450 nm range was obtained by focusing the 800 nm probe beam into a CaF_2 crystal mounted on a rotating holder. An optical chopper was used to modulate the excitation beam at 100 Hz frequency and obtain the value of the TA signal. The relative polarization between the pump and probe beams was set at the magic angle (54.7°). The pump and probe beams were overlapped in the sample. The flow cell (Spectrocell Inc., 0.7 mL volume with 2 mm path length), pumped by a Fluid Metering RHSY Lab pump (Scientific Support Inc.), was used to prevent photodegradation of the sample. After passing through the flow cell, the continuum was coupled into an optical fiber and input into a CCD spectrograph (Ocean Optics, S2000). The data acquisition was achieved using in-house LabVIEW (National Instruments) software routines.

Results and Discussion

Synthesis and Molecular Design. Chart 1 illustrates the structures of the complexes that are the focus of the present investigation. The complexes were synthesized using an iterative-convergent method that relies on the use of orthogonal

TABLE 1: Photophysical Data of Ground-State Absorption and Photoluminescence

	UV−vis λ_{abs}/nm (log ε)	λ_{fl}/nm	λ_{ph}/nm	Φ_{ph}/%
DPAF-Pt	378 (4.78)	392	531	1.1
Pt2[a]	355 (4.85)	374	516	5.2
Pt3[a]	363 (5.10)	386	517	5.8
DPAF-Pt1-NDI	380 (5.16)	391	—[b]	–
	362 (5.05)			
DPAF-Pt2-NDI	380 (5.21)	391	–	–
	363 (5.13)			
DPAF-Pt3-NDI	379 (5.28)	391	–	–
	363 (5.20)			

[a] Reference 19. [b] Phosphorescence was not observed.

alkyne protecting groups as we have previously reported.[19,22] Detailed descriptions of the synthesis and spectroscopic characterization is provided as Supporting Information.

Each complex features three molecular units: (1) (diphenylamino)-2,7-fluorenylene (DPAF), which serves as a primary light absorbing chromophore and an electron donor; (2) the conjugated platinum acetylide "spacer", $[-Pt(PBu_3)_2-C\equiv C-Ph-C\equiv C-]_n$, which also serves as a light absorbing chromophore and an electron donor/acceptor unit; (3) the naphthalenediimide (NDI) unit, which serves as an electron acceptor. In addition to these "primary" functions, the individual units have special features that are of interest in this study. First, the DPAF moiety has been studied extensively as an active element in π-conjugated chromophores that display high-cross section two-photon (2PA) absorption in the near-infrared region.[26−28] The DPAF unit has been studied in a variety of organic chromophores, and more recently in organometallic systems,[29] and it typically augments the 2PA absorption cross section in the 600−800 nm region. Given this precedent, we anticipated it would be possible to excite **DPAF-Ptn-NDI** via a two-photon absorption in this wavelength region. Second, in addition to serving as a spacer, the platinum acetylide moiety exhibits rich photophysical properties.[19,21,30−32] As discussed below, the platinum acetylide conjugated system exhibits allowed π,π^* absorption in the near-UV region, and due to the heavy platinum centers, following excitation the chromophore undergoes rapid intersystem crossing ($\tau \leq 5$ ps).[33] The triplet excited state can be observed by its structured, mid-visible phosphorescence emission and intense visible region transient absorption.[21,34] Finally, the NDI moiety has been employed as an electron acceptor in a series of intramolecular dyads and triads designed to study electron transfer processes.[35] The unit undergoes two reversible one-electron reductions at relatively low cathodic potentials to afford the radical anion $NDI^{\bullet-}$ and the dianion NDI^{2-}. The absorption spectrum of the anion radical state $NDI^{\bullet-}$ exhibits distinct bands in the visible region, providing a convenient probe for its formation and dynamics in photoinduced electron transfer reactions.[35]

Absorption and Emission Spectroscopy. The absorption and emission spectroscopy of the **DPAF-Ptn-NDI** ($n = 1, 2, 3$) complexes were measured to characterize the processes that occur upon light absorption. Important reference data are available from the model compounds **DPAF-Pt**, **Pt2**, and **Pt3**, and some of this data were reported previously.[21,29] A summary of the data is provided in Table 1.

The **DPAF-Ptn-NDI** complexes exhibit absorption in the UV region, with a strong band resolved at 380 nm and a shoulder at 362 nm. The reference complexes **DPAF-Pt**, **Pt2**, and **Pt3** also exhibit strong absorption in the same near-UV wavelength region. For **DPAF-Pt**, the near-UV absorption is primarily due to a π,π^* transition localized on the DPAF unit. For the platinum acetylide oligomers **Pt2** and **Pt3** the near-UV absorption is again due to a π,π^* transition, in this case arising from the π-conjugated $[-Pt(PR_3)_2-C\equiv C-Ph-C\equiv C-]_n$ chromophore.[21] Note that for the **DPAF-Ptn-NDI** series as the spacer length (n) increases from 1 to 3 units the molar absorptivity (ε) increases. This is due to the increase in the length of the $[-Pt(PR_3)_2-C\equiv C-Ph-C\equiv C-]_n$ spacer unit and is consistent with previous studies of platinum acetylide oligomers,[19,21] which indicate that the absorptivity of the π,π^* transition for this chromophore increases with conjugation length. Taken together, the absorption data indicate that for the **DPAF-Ptn-NDI** series, the near-UV absorption arises from a superposition of the absorption by the DPAF chromophore and the $[-Pt(PR_3)_2-C\equiv C-Ph-C\equiv C-]_n$ unit. Thus excitation of the complexes in this wavelength region is anticipated to create excitons that are localized on the DPAF moiety as well as on the $[-Pt(PR_3)_2-C\equiv C-Ph-C\equiv C-]_n$ segment.

Photoluminescence spectroscopy was carried out on the **DPAF-Ptn-NDI** series and the model complexes to provide insight regarding the active excited states. The emission experiments were carried out under air-saturated and degassed conditions to make it possible to distinguish fluorescence and phosphorescence (fl and ph, respectively), the latter of which is quenched in air-saturated solution. First, as a point of reference it is important to note that **DPAF-Pt** exhibits weak fluorescence with $\lambda_{max} \sim 392$ nm and phosphorescence $\lambda_{max} \sim 531$ nm. The fluorescence is very weak, while the phosphorescence has a modest quantum yield, with $\Phi_{ph} \sim 1\%$. These emissions arise from $^1\pi,\pi^*$ and $^3\pi,\pi^*$ states localized primarily on the DPAF chromophore.[21,29] The photoluminescence of the **Pt2** and **Pt3** oligomers has been carefully characterized in previous work,[19,21] which reveals that the conjugated $[-Pt(PR_3)_2-C\equiv C-Ph-C\equiv C-]_n$ chromophore features weak fluorescence in the near-UV and moderately efficient phosphorescence with $\lambda \sim 517$ nm. For each of the model systems, the fluorescence is weak because intersystem crossing is rapid, giving rise to production of the triplet state with near unit quantum efficiency. The phosphorescence that is observed for **DPAF-Pt** and the **Pt2** and **Pt3** complexes allows us to pinpoint the triplet energies for the DPAF and $[-Pt(PR_3)_2-C\equiv C-Ph-C\equiv C-]_n$ chromophores as 2.40 and 2.33 eV, respectively.

The **DPAF-Ptn-NDI** series exhibit only very weak fluorescence ($\Phi_{fl} < 0.005$) at a wavelength corresponding to the fluorescence observed from **DPAF-Pt**. Importantly, phosphorescence emission is not observed from the **DPAF-Ptn-NDI** complexes. Compared with the phosphorescence of **DPAF-Pt** ($\Phi_p = 1.1\%$), **Pt2** ($\Phi_p = 5.2\%$), and **Pt3** ($\Phi_p = 5.8\%$), the absence of phosphorescence in **DPAF-Ptn-NDI** indicates nearly quantitative quenching of the triplet excited state by an efficient nonradiative processes. As discussed below, this nonradiative decay channel is believed to be photoinduced charge transfer.

Electrochemistry. The electrochemical response of the **DPAF-Ptn-NDI** ($n = 1, 2, 3$) series was determined by cyclic voltammetry experiments carried out in nitrogen-saturated dichloromethane solution with 0.1 M tetrabutylammonium hexafluorophosphate (TBAH). The ferrocene/ferrocenium couple was used as internal standard, and the listed potentials are converted to the saturated calomel electrode using the value $E_{1/2}(Fc^+/Fc) = 0.43$ V vs SCE.[36] The electrochemistry of **Pt2**, **Pt3**, and **Pt-NDI** was reported previously,[20,22] while the response of **DPAF-Pt** was characterized as part of this work. A summary of the relevant potentials is provided in Table 2. The cyclic voltammograms for the **DPAF-Ptn-NDI** complexes ($n = 1 - 3$) were essentially identical (see Supporting Information for

TABLE 2: Redox Potentials (V vs SCE) in CH_2Cl_2 Solution

	$E_{ox}(1)$	$E_{red}(1)$	$E_{red}(2)$
Pt2[a]	0.89		
Pt3[a]	0.85		
DPAF-Pt	0.72[b]		
NDI-Pt		−0.62	−1.02
DPAF-Pt1-NDI	0.71[b]	−0.63	−1.03
DPAF-Pt2-NDI	0.72[b]	−0.62	−1.02
DPAF-Pt3-NDI	0.71[b]	−0.63	−1.04

[a] Reference 20. [b] Irreversible wave.

cyclic voltammograms). Each complex exhibits a quasi-reversible anodic wave at ~0.72 V, and two reversible cathodic waves at −0.62 and −1.02 V. Comparison of these potentials with the waves observed for the reference compounds **DPAF-Pt** and **Pt-NDI** indicates that the anodic wave corresponds to an oxidation process localized primarily on the DPAF unit, whereas the two cathodic waves correspond to sequential one-electron reductions localized the NDI acceptor moiety. The potential observed for reduction of the NDI acceptor unit in the **DPAF-Ptn-NDI** series are consistent with previous electrochemical studies of compounds that contain similar molecular units.[35] This result indicates that the redox properties of the donor and acceptor units are not strongly perturbed by being incorporated into the platinum acetylide donor−acceptor architecture.

It is also important to note that in previous work we have characterized the electrochemical response of **Pt2** and **Pt3** as part of a comprehensive study of the properties of radical ions of platinum acetylide oligomers. This work reveals that the $[-Pt(PR_3)_2-C\equiv C-Ph-C\equiv C-]_n$ conjugated system is oxidized at $E_{1/2} \sim 0.87$ V. The cyclic voltammograms for the **DPAF-Ptn-NDI** series did not exhibit a clearly resolved wave that could be assigned to this process (see Figure 2 in Supporting Information). However, given the structural similarity of the $[-Pt(PR_3)_2-C\equiv C-Ph-C\equiv C-]_n$ moiety in the **DPAF-Ptn-NDI** series and **Pt2** (or **Pt3**), we anticipate that the platinum acetylide spacer is oxidized at a similar potential in the donor−acceptor complexes.

Transient Absorption Spectroscopy. Detailed insight into the processes that occur in the **DPAF-Ptn-NDI** complexes is provided by transient absorption (TA) experiments carried out on the nanosecond (ns) and picosecond (ps) time scales. These experiments were carried out using different instruments, and the results are described separately below.

Initial studies were carried out on an instrument that provides near-UV/visible region transient spectra with 5 ns time resolution with excitation provided by the 355 nm output of a Q-switched Nd:YAG laser (5 mJ pulse energy, 5 ns fwhm). The TA spectra of the **DPAF-Ptn-NDI** complexes obtained on this instrument are shown in Figure 1. The spectra for the three complexes are identical, except for a small difference in the decay rate for the transient. The difference absorption spectra feature broad absorption in the visible region with a peak at $\lambda \sim 476$ nm, a shoulder at $\lambda \sim 524$ nm, and a weak band at $\lambda \sim 604$ nm. For each complex the absorption decays uniformly across the entire spectrum, and the decay lifetime (τ_{CR}) is slightly longer for the $n = 2$ and 3 oligomers (10, 31, and 25 ns for $n = 1$, 2, and 3, respectively).

There are several features that make it clear the transient observed for the **DPAF-Ptn-NDI** complexes is the charge separated state in which an electron hole is located on the DPAF donor and the electron is located on the NDI acceptor, i.e., $DPAF^{\bullet+}$-Ptn-$NDI^{\bullet-}$. First, previous studies of platinum acetylide

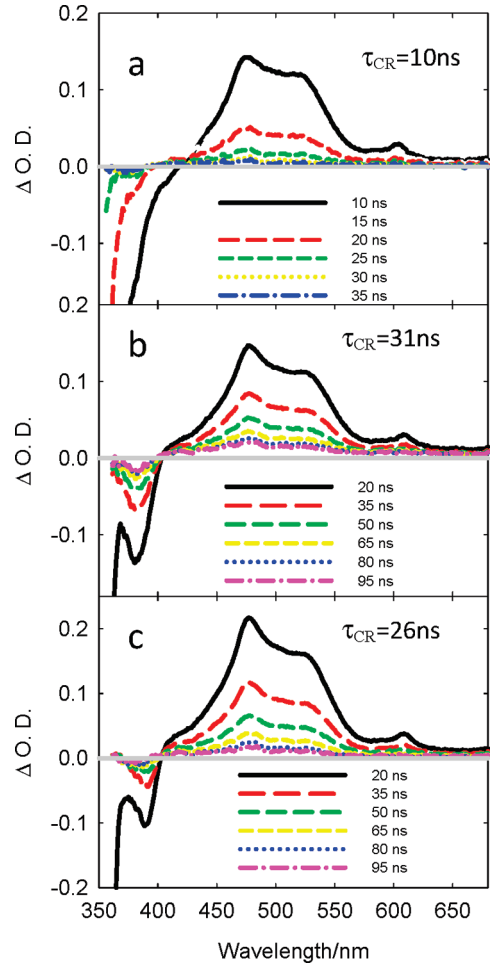

Figure 1. Transient absorption difference spectra of **DPAF-Ptn-NDI** complexes in argon-purged THF: (a) **DPAF-Pt1-NDI**; (b) **DPAF-Pt2-NDI**; (c) **DPAF-Pt3-NDI**. Excitation at 355 nm, ca. 10 mJ/pulse.

oligomers and polymers show that the singlet and triplet excited states for the $[-Pt(PR_3)_2-C\equiv C-Ph-C\equiv C-]_n$ chromophore exhibit broad, structureless bands in the 600−700 nm region.[19,34,37,38] In addition, the triplet state is long-lived, with lifetimes >5 μs typical.[34,38] Thus, the difference in spectral shape and (short) lifetime observed for the **DPAF-Ptn-NDI** complexes argues against the spectrum arising from the singlet or triplet states. Second, spectroelectrochemical work carried out by Wasielewski and co-workers show that $NDI^{\bullet-}$ features absorption bands at 476 and 604 nm in relative intensity ratios that are the same as those observed in the transient spectra of the **DPAF-Ptn-NDI** complexes.[35] Finally, as outlined in detail below, the band that appears as a shoulder at 524 nm in the **DPAF-Ptn-NDI** TA spectra likely arises from the oxidized donor, $DPAF^{\bullet+}$.

To provide insight into the absorption spectrum of the oxidized donor unit, $DPAF^{\bullet+}$, a bimolecular electron transfer quenching experiment was carried out using the model complex **DPAF-Pt** and *N*,*N*′-dimethyl-4,4′-bipyridinium ($\mathbf{MV^{2+}}$) as an electron transfer quencher. A solution containing **DPAF-Pt** and $\mathbf{MV^{2+}}$ was excited at 355 nm using the Nd:YAG laser, and Figure 2 illustrates the time-resolved absorption-difference spectra that were observed for this system. At initial times after excitation, the spectrum is dominated by a broad absorption with $\lambda \sim 600$ nm. This transient is the triplet excited state of **DPAF-Pt**. Over a time course of ca. 1 μs the spectrum evolves into a more complex set of absorptions in the near-UV and visible range. This spectral evolution is due to

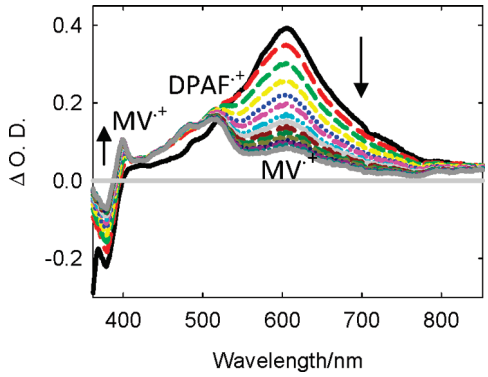

Figure 2. Transient absorption difference spectra of **DPAF-Pt** and $\mathbf{MV^{2+}}$ in THF/MeCN (2:1) solution. The solution of **DPAF-Pt** was prepared with optical density of 0.7 at 355 nm ($c \sim 50\ \mu$M), and the concentration of $\mathbf{MV^{2+}}$ was 0.1 mM. Excitation at 355 nm, ca. 10 mJ/pulse. Spectra obtained at delay increments of 100 ns.

bimolecular photoinduced electron transfer from the triplet state of the donor to the acceptor, eq 1.[39]

$$^3\mathbf{DPAF\text{-}Pt^*} + \mathbf{MV^{2+}} \rightarrow \mathbf{DPAF\text{-}Pt^{\bullet+}} + \mathbf{MV^{\bullet+}} \quad (1)$$

Given this reaction, it is straightforward to assign the various bands seen in the transient spectrum after the initial spectral evolution is complete (~1.4 μs). Thus, the narrow peak at 395 nm and broad, weaker band at 604 nm is due to the reduced acceptor, $MV^{\bullet+}$.[40] By inference, the strong band with $\lambda_{max} \sim 510$ nm and a shoulder at 485 nm is assigned to the absorption of the $DPAF^{\bullet+}$ moiety in the oxidized complex **DPAF-Pt**$^{\bullet+}$.

Given that we have access to the spectrum of $NDI^{\bullet+}$ from literature spectroelectrochemical data,[35] and the spectrum of $DPAF^{\bullet+}$ from the results shown in Figure 2, we decided to simulate the spectrum of the $DPAF^{\bullet+}$-Ptn-$NDI^{\bullet-}$ charge separated state. The simulation was carried out by adding together the spectrum of $NDI^{\bullet+}$ (obtained by digitizing Figure 1 from ref 35) and the long-time spectrum from the **DPAF-Pt/**$\mathbf{MV^{2+}}$ bimolecular quenching experiment (Figure 2). The individual spectra that were used in the summation are plotted in Figure 3a. The relative weight of these two spectra was adjusted to optimize the fit to the TA spectrum of **DPAF-Pt2-NDI** (Figure 1b). The results of the optimized fit are compared to the TA spectrum of **DPAF-Pt2-NDI** in Figure 3b. Here it is evident the fit is quite good, with the exception for deviation in the fitted spectrum at $\lambda < 420$ nm and at $\lambda \sim 600$ nm, which are the regions where $\mathbf{MV^{\bullet+}}$ absorbs in the **DPAF-Pt/**$\mathbf{MV^{2+}}$ bimolecular quenching experiment. The excellent agreement between the fitted and observed spectra provides compelling evidence for assignment of the transients observed following excitation of **DPAF-Ptn-NDI** to the charge separated state.

To provide insight concerning the mechanism and dynamics for formation of the charge separated states in the both **DPAF-Ptn-NDI** complexes, transient absorption experiments were carried out using a system with 100 fs pulsed excitation at 400 nm. These experiments were done with **DPAF-Pt2-NDI** and **DPAF-Pt3-NDI**, and the time-resolved spectral data were essentially identical (although the kinetics differed, see below). For this reason herein we only show the time-resolved spectral data for **DPAF-Pt2-NDI**.

Figure 4a illustrates the time-resolved absorption data for **DPAF-Pt2-NDI** in THF following ~100 fs excitation. At early delay times (5−100 ps), the spectra are dominated by broad absorption between 600−700 nm that arises from the triplet

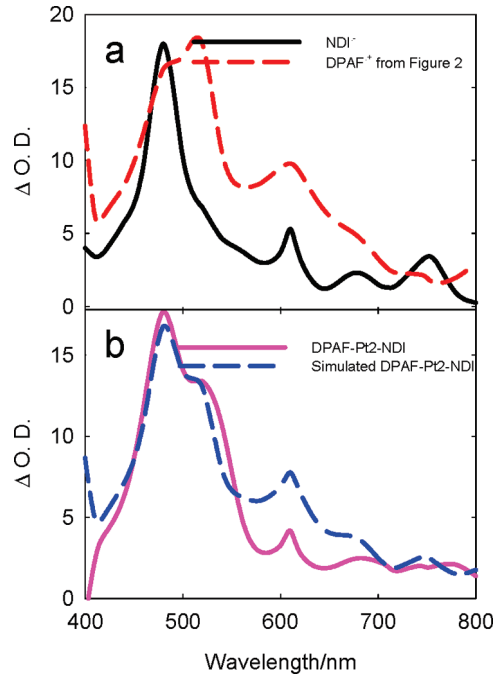

Figure 3. (a) Black-solid: absorption spectrum of **NDI** radical anion (from ref 35). Red-dashed: absorption of **DPAF** radical cation (from Figure 2 at long delay time). (b) Pink: transient absorption difference spectrum of **DPAF-Pt2-NDI** in THF. Blue: weighted sum of **NDI** radical anion and **DPAF** radical cation spectra from part a of figure.

excited state localized either on the DPAF or $[-Pt(PR_3)_2-C\equiv C-Ph-C\equiv C-]_n$ chromophores.[21,29] The inset of Figure 4a shows an expansion of the time-resolved spectra over the 420−800 nm region over a period of ~1 ns following excitation. The spectral evolution can be clearly seen here, where the triplet absorption band at 600−700 nm decays concomitant with the appearance of the spectral features characteristic of the charge separated state at 476, 520, and 604 nm. Figure 4b shows the transient absorption dynamics at 480 and 680 nm for **DPAF-Pt2-NDI**. At 680 nm, at very early times ($t < 5$ ps), there is a rapid decay arising from singlet−triplet intersystem crossing.[33,41] (This is evident as the "spike" in the 680 nm kinetic trace in Figure 4b; see Supporting Information Figure 4 for more detail). Following this prompt component, the triplet absorption at 680 nm decays with the same first-order rate constant as the rise of the absorption due to the charge separated state when monitored at 480 nm ($k = 1.3 \times 10^9\ s^{-1}$). The coincidence of the triplet decay and rise of the charge separated state indicates that there are no intermediates observable. The significance of this result will be discussed further below. As noted above, the overall spectral changes observed for **DPAF-Pt3-NDI** are essentially the same, as shown in Figure 4a; however, for this complex the triplet decay and charge separated state rise occur with $k = 8.4 \times 10^8\ s^{-1}$, which is ~30% slower than for **DPAF-Pt2-NDI**.

Two-Photon Excitation of the Charge Separated State. In previous investigations, we and others have shown that platinum acetylide chromophores exhibit pronounced nonlinear absorption of short (femtosecond) and long (nanosecond) laser pulses in the 600−800 nm wavelength region.[29,42−46] In many cases it has been shown that the nonlinear absorption arises from simultaneous two-photon absorption (2PA) resulting in direct production of the lowest singlet state (and ultimately the triplet excited state following intersystem crossing). Structure−activity studies have shown that the incorporation of conjugated donor-π-spacer "ligands" such as DPAF into the structure enhances

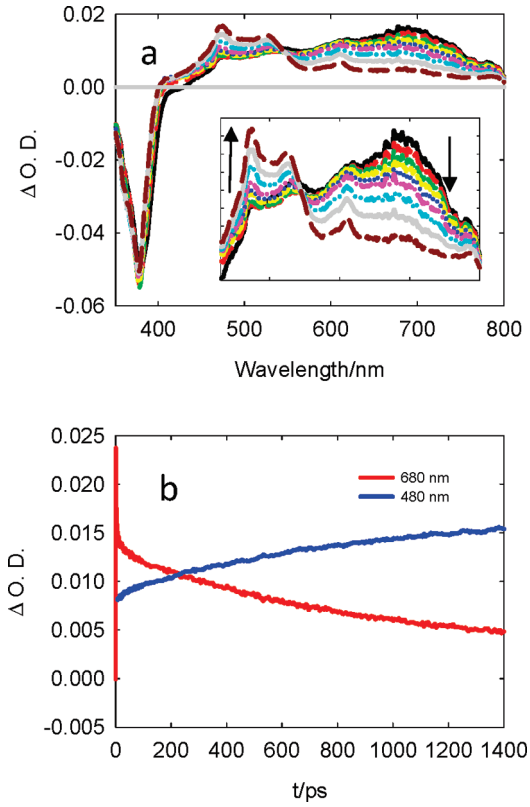

Figure 4. (a) Picosecond transient absorption spectra of 0.025 mM **DPAF-Pt2-NDI** in THF solution. The sample was excited with a 5 μJ/pulse pump beam at 400 nm and probed using white-light continuum. The delay times range from 10 to 500 ps. The inset shows the spectral changes occurring in the 400−750 nm region; arrows show the direction of change in the spectra with increasing delay time. (b) Transient absorption kinetics monitored at 680 nm (red plot, decaying absorption) and 480 nm (blue plot, increasing absorption).

the efficiency of nonlinear absorption by increasing the effective cross section for 2PA.

Given the structural similarity of the **DPAF-Ptn-NDI** complexes with other platinum acetylide chromophores that have been shown to exhibit efficient 2PA in the near-infrared region, we set out to determine if it would be possible to use 2PA to excite the complexes. In this case, we anticipated that on a nanosecond time scale 2PA excitation would result in the appearance of the charge separated state, since intersystem crossing and production of the charge separated state have been shown to occur within 1 ns following initial excitation (under 1 photon excitation conditions). Experiments were carried out with the series of **DPAF-Ptn-NDI** complexes dissolved in THF solution at a concentration of 5 mM. The samples were excited at 618 nm using the output of an OPO pumped by a Q-switched Nd:YAG laser. Importantly, the ground-state absorption by the complexes at 618 nm is negligible, so at this wavelength we anticipate that any excitation must result from direct 2PA absorption. Similar results were obtained for the series of three **DPAF-Ptn-NDI** complexes, so here we only show the data for **DPAF-Pt2-NDI**. Figure 5 illustrates the transient absorption spectrum obtained when a sample of **DPAF-Pt2-NDI** is excited with 618 nm excitation pulses. Although the transient absorption signal is weak, there is a clearly resolved absorption with $\lambda_{max} \sim 476$ nm and a shoulder at $\lambda \sim 524$ nm. (The spectrum below 440 nm is obscured due to strong ground-state absorption, and above 575 nm due to the scattered excitation light.) It is seen that the transient absorption spectral band shape obtained with excitation in the red matches closely with that observed with near-

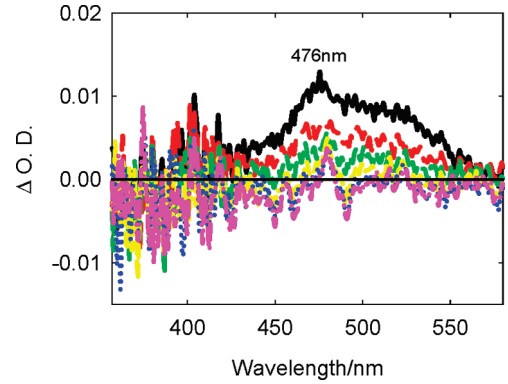

Figure 5. Two-photon excited transient absorption spectrum of **DPAF-Pt2-NDI** in THF. Excitation at 618 nm with the focused output of an OPO pumped by a Nd/YAG laser.

UV excitation. This supports the notion that the charge separated state can be produced by 2PA excitation of **DPAF-Pt2-NDI**.

To understand the significance of this demonstration of two-photon excited charge separation, it is important to put this work into context. Two-photon absorption materials have potential applications such as optical data storage,[47,48] optical limiting materials,[49,50] lasers,[51] fluorescence imaging,[52] photodynamic therapy,[53] and 3D microfabrication.[54,55] Two-photon excited electron transfer has been used in photolithography to provide subwavelength resolution.[56] The advantages of a two-photon induced electron transfer include (1) the ability to use low-energy (near-infrared) photons making the photosystem less susceptible to photodegradation effects and (2) better tissue penetration for in vivo biological applications. In our **DPAF-Ptn-NDI** system, intramolecular electron transfer is demonstrated to occur under two-photon excitation at 618 nm. Moreover, on the basis of recent work on structurally related DPAF-substituted platinum acetylides it is clear that 2PA excitation of the **DPAF-Ptn-NDI** complexes is possible at even longer wavelengths (700−900 nm).[29,57] Thus, this work provides a pathway for the design of donor−acceptor systems that can be used to drive electron transfer processes under near-infrared excitation for a variety of materials or biological applications.

Mechanism and Energetics of Photoinduced Charge Transfer. To fully understand the processes that occur following excitation of the **DPAF-Ptn-NDI** complexes, it is necessary to map the energies of the lowest excited and charge separated states. The information needed for this analysis is available from the spectroscopic and electrochemical data (Tables 1 and 2). For this analysis the state energies and redox potentials for **DPAF-Pt2-NDI** are used, but the values are not significantly different for the $n = 1$ or 3 complexes.

Figure 6 summarizes the energies of the excited and charge separated states for **DPAF-Pt2-NDI**. First, there are $^1\pi,\pi^*$ states concentrated on the DPAF and/or $[-Pt(PR_3)_2-C\equiv C-Ph-C\equiv C-]_n$ chromophores. As discussed above, the energies of these states are similar (~3.15−3.20 eV), so it is likely that the initially created exciton is distributed (or delocalized) between the chromophores. Next, there are corresponding $^3\pi,\pi^*$ states, again localized on the two chromophores at 2.33 and 2.40 eV for DPAF and $[-Pt(PR_3)_2-C\equiv C-Ph-C\equiv C-]_n$, respectively. There are two distinct charge separated states, both of which lie below the energies of the $^1\pi,\pi^*$ and $^3\pi,\pi^*$ states. The first state (CS_1) is at ~1.51 eV and has the electron on the NDI acceptor and the electron−hole localized on the $[-Pt(PR_3)_2-C\equiv C-Ph-C\equiv C-]_n$ spacer. The second state (CS_2) is at ~1.34 eV and has the electron localized on the NDI acceptor and the electron−hole on the DPAF moiety.[58]

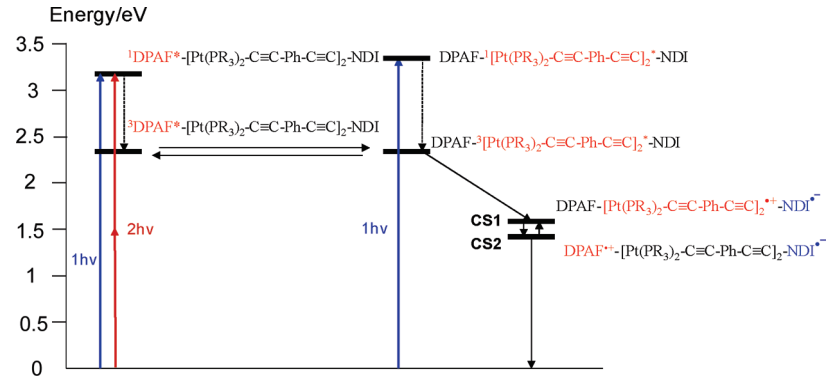

Figure 6. Energy level diagram for **DPAF-Pt2-NDI**. Energies based on spectroscopic and electrochemical data are as described in text.

With the energies of the various states in mind, we now consider the events that occur following excitation of the **DPAF-Ptn-NDI** complexes. Initial one- or two-photon excitation produces the manifold of $^1\pi,\pi^*$ states based on the DPAF and $[-Pt(PR_3)_2-C\equiv C-Ph-C\equiv C-]_n$ chromophores. Rapid intersystem crossing then occurs to produce the $^3\pi,\pi^*$ state.[33] In previous studies of platinum acetylide chromophores it has been shown that in complexes of the type, L_1-Pt(P)$_2$-L_2, where P is a phosphine ligand and L_1 and L_2 are π-conjugated ligands, the triplet exciton is localized on one of the ligands (L_1 or L_2).[59] Moreover, in cases where the ligand based triplet energies are similar, the two localized triplets are in equilibrium.[60] In the **DPAF-Ptn-NDI** complexes the triplets localized on the DPAF and $[-Pt(PR_3)_2-C\equiv C-Ph-C\equiv C-]_n$ chromophores are close in energy. Thus, it is likely that the triplet exists as an equilibrium distribution of two $^3\pi,\pi^*$ states localized on the two chromophores, with equilibrium favoring the ^{3}DPAF* state, which is 0.07 eV lower in energy. Given the relatively large separation distance between the DPAF and NDI units (25−50 Å) it is unlikely that direct photoinduced charge transfer from ^{3}DPAF* to NDI occurs to produce CS_2. It is more probable that the process occurs stepwise, with initial transfer from the $[-Pt(PR_3)_2-C\equiv C-Ph-C\equiv C-]_n$ triplet state to NDI to produce CS_1 in which the electron is on the NDI acceptor and the hole is on the $[-Pt(PR_3)_2-C\equiv C-Ph-C\equiv C-]_n$ spacer. Subsequently, a charge shift process occurs in which the electron hole moves from the $[-Pt(PR_3)_2-C\equiv C-Ph-C\equiv C-]_n$ spacer to DPAF to produce CS_2 (see eq 2).

A summary of the observed rate constants for charge separation (k_{CS}) and charge recombination (k_{CR}) is provided in Table 3. Importantly, these are observed rates, and as outlined below, since charge separation and recombination likely occur by (hole) hopping across the bridge, the observed rate constants likely do not correspond to microscopic rates of electron or hole transfer. The ultrafast transient absorption results provide considerable insight into the charge separation process (Figure 4). In particular, the time-resolved data show that the absorption of the triplet state evolves directly into the absorption of CS_2 (with isosbestic points). This result indicates that the population of CS_1 does not build up to any extent. Another interesting point is that the rates of charge separation are comparatively slow ($\sim 10^9$ s^{-1}), and they do not vary much with the spacer length. This is surprising, given the comparatively large driving force for charge separation, $\Delta G \sim -0.8$ eV. A possible explanation for this result is that the excited-state equilibrium favors the DPAF localized triplet, and thus charge separation requires initial population of the (higher energy) $[-Pt(PR_3)_2-C\equiv C-Ph-C\equiv C-]_n$ localized triplet followed by photoinduced electron transfer, eq 2:

$$\begin{array}{c} \mathbf{^3DPAF^*}\text{-}[-Pt(PR_3)_2-C\equiv C-Ph-C\equiv C-]_n\text{-NDI} \rightleftharpoons \text{DPAF-}\mathbf{^3[-Pt(PR_3)_2-C\equiv C-Ph-C\equiv C-]_n}^*\text{-NDI} \rightarrow \\ \text{DPAF-}\mathbf{[-Pt(PR_3)_2-C\equiv C-Ph-C\equiv C-]_n^{\bullet+}\text{-}NDI^{\bullet-}} \rightarrow \mathbf{DPAF^{\bullet+}}\text{-}[-Pt(PR_3)_2-C\equiv C-Ph-C\equiv C-]_n\text{-}\mathbf{NDI^{\bullet-}} \\ \mathbf{CS_1} \qquad\qquad\qquad\qquad\qquad\qquad\qquad\qquad\qquad\qquad\qquad\qquad \mathbf{CS_2} \end{array} \quad (2)$$

Since the equilibrium favors ^{3}DPAF*, the initial step of charge separation involves triplet hopping to produce the bridge triplet, and this process is comparatively slow ($k \sim 10^9$ s^{-1}) because it is slightly endothermic. This is the probable explanation as to why the observed charge separation rates are relatively low and do not vary much with the length of the $[-Pt(PR_3)_2-C\equiv C-Ph-C\equiv C-]_n$ bridge.

Finally, we consider the mechanism of charge recombination. As noted above, the observed rates do not vary much across the **DPAF-Ptn-NDI** series (Table 3). This finding argues against the process occurring via a direct, bridge-mediated (superexchange) electron (or hole) transfer mechanism. In contrast, it is consistent with a stepwise hole-hopping process involving CS_1 as an intermediate, eq 3.

$$\begin{array}{c} \mathbf{DPAF^{\bullet+}}\text{-}[-Pt(PR_3)_2-C\equiv C-Ph-C\equiv C-]_n\text{-}\mathbf{NDI^{\bullet-}} \rightarrow \text{DPAF-}\mathbf{[-Pt(PR_3)_2-C\equiv C-Ph-C\equiv C-]_n^{\bullet+}}\text{-NDI}^{\bullet-} \rightarrow \\ \mathbf{CS_2} \qquad\qquad\qquad\qquad\qquad\qquad\qquad\qquad\qquad\qquad\qquad\qquad \mathbf{CS_1} \\ \text{DPAF-}[-Pt(PR_3)_2-C\equiv C-Ph-C\equiv C-]_n\text{-NDI} \end{array} \quad (3)$$

In this case, the spacer serves as a "molecular wire", facilitating charge recombination via direct injection of the hole into the π-conjugated $[-Pt(PR_3)_2-C\equiv C-Ph-C\equiv C-]_n$ electronic system. Even though the cation charge state in the $[-Pt(PR_3)_2-C\equiv C-Ph-C\equiv C-]_n$ system is spatially confined,[20] its ability to rapidly hop between repeat units gives rise to a weakly distant dependent charge recombination rate. Distance independent rates were observed by Wasielewski and co-workers for charge recombination across π-conjugated π-phenylene oligomers, and they also attributed the weak distance dependence to direct involvement of bridge-localized hole states in the mechanism.[15]

TABLE 3: Dynamics of Charge Separation and Charge Recombination

	$k_{CS}/10^9$ s^{-1}	$k_{CR}/10^7$ s^{-1}
DPAF-Pt1-NDI		10
DPAF-Pt2-NDI	1.3	3.2
DPAF-Pt3-NDI	0.84	3.8

Summary and Conclusion

This study has examined excited-state spectroscopy and dynamics in the series of platinum acetylide oligomers **DPAF-Ptn-NDI** that are end-functionalized with DPAF electron donor and NDI electron acceptor units. These complexes were developed to allow the study of photoinduced charge separation across the platinum acetylide "spacer", $[-Pt(PR_3)_2-C\equiv C-Ph-C\equiv C-]_n$. This structure is of interest as it is a prototypical example of an organometallic π-conjugated system which relies on dπ-(metal)−pπ-(carbon) overlap. Steady-state photoluminescence spectroscopy reveals that the fluorescence and phosphorescence characteristics of the DPAF and $[-Pt(PR_3)_2-C\equiv C-Ph-C\equiv C-]_n$ chromophores are entirely quenched in the **DPAF-Ptn-NDI** complexes, indicating that there is a rapid, nonradiative channel operating. Nanosecond transient absorption spectroscopy reveals the existence of a transient assigned to the charge separated state in which the DPAF unit is oxidized and the NDI acceptor is reduced, DPAF$^{\bullet+}$-Ptn-NDI$^{\bullet-}$. Picosecond transient absorption spectroscopy finds that the charge separated state is produced directly from a triplet excited state with a rate $k \sim 10^9$ s^{-1} that does not vary strongly with the length of the $[-Pt(PR_3)_2-C\equiv C-Ph-C\equiv C-]_n$ spacer. Charge recombination is also relatively rapid ($k \sim 3 \times 10^7$ s^{-1}), and the rate also does not change much with spacer length. Taken together, the results suggest that charge separation and charge recombination occur via stepwise, hole hopping pathways that involve intermediate states in which the $[-Pt(PR_3)_2-C\equiv C-Ph-C\equiv C-]_n$ spacer is oxidized. Even though the positive polaron state on the bridge is relatively localized, rapid hopping of the polaron between repeat units on the longer $[-Pt(PR_3)_2-C\equiv C-Ph-C\equiv C-]_n$ spacer leads to efficient charge transport.

Acknowledgment. The work done at the University of Florida was supported by the National Science Foundation (Grant No. CHE-0515066) and the Air Force Office of Scientific Research (FA9550-09-1-0186). K.D.G. acknowledges the Ohio Laboratory for Kinetic Spectroscopy (BGSU) for providing the resources needed to perform ultrafast measurements. J.E.Y. was supported by the Air Force Institute of Technology (AFIT).

Supporting Information Available: Complete details of the synthesis and structural characterization of all compounds (including NMR spectral data for **DPAF-Ptn-NDI** complexes), UV−visible absorption spectra, cyclic voltammetry, and GPC analysis traces. This material is available free of charge via the Internet at http://pubs.acs.org.

References and Notes

(1) Wasielewski, M. R. *Chem. Rev.* **1992**, *92*, 435–461.
(2) Chen, P.; Meyer, T. J. *Chem. Rev.* **1998**, *98*, 1439–1478.
(3) Wasielewski, M. R.; Niemczyk, M. P.; Svec, W. A.; Pewitt, E. B. *J. Am. Chem. Soc.* **1985**, *107*, 1080–1082.
(4) Gaines, G. L.; O'Neil, M. P.; Svec, W. A.; Niemczyk, M. P.; Wasielewski, M. R. *J. Am. Chem. Soc.* **1991**, *113*, 719–721.
(5) Davis, W. B.; Svec, W. A.; Ratner, M. A.; Wasielewski, M. R. *Nature* **1998**, *396*, 60–63.
(6) Seta, P.; Bienvenue, E.; Moore, A. L.; Mathis, P.; Bensasson, R. V.; Liddell, P.; Pessiki, P. J.; Joy, A.; Moore, T. A.; Gust, D. *Nature* **1985**, *316*, 653–5.
(7) Dixon, I. M.; Collin, J.-P.; Sauvage, J.-P.; Barigelletti, F.; Flamigni, L. *Angew. Chem., Int. Ed.* **2000**, *39*, 1292–1295.
(8) Ballardini, R.; Balzani, V.; Clemente-Leon, M.; Credi, A.; Gandolfi, M. T.; Ishow, E.; Perkins, J.; Stoddart, J. F.; Tseng, H.-R.; Wenger, S. *J. Am. Chem. Soc.* **2002**, *124*, 12786–12795.
(9) Wallin, S.; Monnereau, C.; Blart, E.; Gankou, J. R.; Odobel, F.; Hammarstrom, L. *J. Phys. Chem. A* **2010**, *114*, 1709–1721.
(10) Wilson, T. M.; Tauber, M. J.; Wasielewski, M. R. *J. Am. Chem. Soc.* **2009**, *131*, 8952–8957.
(11) Goldsmith, R. H.; DeLeon, O.; Wilson, T. M.; Finkelstein-Shapiro, D.; Ratner, M. A.; Wasielewski, M. R. *J. Phys. Chem. A* **2008**, *112*, 4410–4414.
(12) Weiss, E. A.; Wasielewski, M. R.; Ratner, M. A. In *Molecular Wires: from Design to Properties*; Springer: Berlin, 2005; Vol. 257, pp 103−133.
(13) Goldsmith, R. H.; Sinks, L. E.; Kelley, R. F.; Betzen, L. J.; Liu, W. H.; Weiss, E. A.; Ratner, M. A.; Wasielewski, M. R. *Proc. Natl. Acad. Sci. U.S.A.* **2005**, *102*, 3540–3545.
(14) Liddell, P. A.; Kodis, G.; Andreasson, J.; de la Garza, L.; Bandyopadhyay, S.; Mitchell, R. H.; Moore, T. A.; Moore, A. L.; Gust, D. *J. Am. Chem. Soc.* **2004**, *126*, 4803–4811.
(15) Weiss, E. A.; Ahrens, M. J.; Sinks, L. E.; Gusev, A. V.; Ratner, M. A.; Wasielewski, M. R. *J. Am. Chem. Soc.* **2004**, *126*, 5577–5584.
(16) Davis, W. B.; Ratner, M. A.; Wasielewski, M. R. *Chem. Phys.* **2002**, *281*, 333–346.
(17) Wolffs, M.; Delsuc, N.; Veldman, D.; Van Anh, N.; Williams, R. M.; Meskers, S. C. J.; Janssen, R. A. J.; Huc, I.; Schenning, A. *J. Am. Chem. Soc.* **2009**, *131*, 4819–4829.
(18) Beckers, E. H. A.; Meskers, S. C. J.; Schenning, A.; Chen, Z. J.; Wurthner, F.; Janssen, R. A. J. *J. Phys. Chem. A* **2004**, *108*, 6933–6937.
(19) Liu, Y.; Jiang, S.; Glusac, K.; Powell, D. H.; Anderson, D. F.; Schanze, K. S. *J. Am. Chem. Soc.* **2002**, *124*, 12412–12413.
(20) Cardolaccia, T.; Funston, A. M.; Kose, M. E.; Keller, J. M.; Miller, J. R.; Schanze, K. S. *J. Phys. Chem. B* **2007**, *111*, 10871–10880.
(21) Glusac, K.; Kose, M. E.; Jiang, H.; Schanze, K. S. *J. Phys. Chem. B* **2007**, *111*, 929–940.
(22) Keller, J. M.; Schanze, K. S. *Organometallics* **2009**, *28*, 4210–4216.
(23) Harriman, A. *J. Chem. Soc., Chem. Commun.* **1977**, 777–778.
(24) Farley, R. T. *Photophysics of Platinum and Iridium Organometallic Materials: From Molecular Wires to Nonlinear Optics*; Ph.D. Dissertation, University of Florida, Gainesville, FL, 2007; http://www.chem.ufl.edu/~kschanze/index_files/Publications.htm.
(25) Nikolaitchik, A. V.; Korth, O.; Rodgers, M. A. J. *J. Phys. Chem. A* **1999**, *103*, 7587–7596.
(26) He, G. S.; Tan, L. S.; Zheng, Q.; Prasad, P. N. *Chem. Rev.* **2008**, *108*, 1245–1330.
(27) Zhou, G. J.; Wong, W. Y.; Poon, S. Y.; Ye, C.; Lin, Z. Y. *Adv. Funct. Mater.* **2009**, *19*, 531–544.
(28) Reinhardt, B. A.; Brott, L. L.; Clarson, S. J.; Dillard, A. G.; Bhatt, J. C.; Kannan, R.; Yuan, L. X.; He, G. S.; Prasad, P. N. *Chem. Mater.* **1998**, *10*, 1863–1874.
(29) Rogers, J. E.; Slagle, J. E.; Krein, D. M.; Burke, A. R.; Hall, B. C.; Fratini, A.; McLean, D. G.; Fleitz, P. A.; Cooper, T. M.; Drobizhev, M.; Makarov, N. S.; Rebane, A.; Kim, K.-Y.; Farley, R.; Schanze, K. S. *Inorg. Chem.* **2007**, *46*, 6483–6494.
(30) Wilson, J. S.; Chawdhury, N.; Al-Mandhary, M. R. A.; Younus, M.; Khan, M. S.; Raithby, P. R.; Köhler, A.; Friend, R. H. *J. Am. Chem. Soc.* **2001**, *123*, 9412–9417.
(31) Wong, W. Y. *Dalton Trans.* **2007**, 4495–4510.
(32) Wilson, J. S.; Kohler, A.; Friend, R. H.; Al-Suti, M. K.; Al-Mandhary, M. R. A.; Khan, M. S.; Raithby, P. R. *J. Chem. Phys.* **2000**, *113*, 7627–7634.
(33) Ramakrishna, G.; Goodson, T.; Rogers-Haley, J. E.; Cooper, T. M.; McLean, D. G.; Urbas, A. *J. Phys. Chem. C* **2009**, *113*, 1060–1066.
(34) Rogers, J. E.; Cooper, T. M.; Fleitz, P. A.; Glass, D. J.; McLean, D. G. *J. Phys. Chem. A* **2002**, *106*, 10108–10115.
(35) Greenfield, S. R.; Svec, W. A.; Gosztola, D.; Wasielewski, M. R. *J. Am. Chem. Soc.* **1996**, *118*, 6767–6777.
(36) Jones, N. D.; Wolf, M. O.; Giaquinta, D. M. *Organometallics* **1997**, *16*, 1352–1354.
(37) Cooper, T. M.; Krein, D. M.; Burke, A. R.; McLean, D. G.; Rogers, J. E.; Slagle, J. E.; Fleitz, P. A. *J. Phys. Chem. A* **2006**, *110*, 4369–4375.
(38) Rogers, J. E.; Hall, B. C.; Hufnagle, D. C.; Slagle, J. E.; Ault, A. P.; McLean, D. G.; Fleitz, P. A.; Cooper, T. M. *J. Chem. Phys.* **2005**, *122*, 214708.
(39) On the basis of the oxidation potential of the **DPAF-Pt**, the reduction potential of MV^{2+} and the triplet energy of **DPAF-Pt**, the free energy of eq 1 is computed to be −1.15 eV.
(40) Kosower, E. M.; Poziomek, E. J. *J. Am. Chem. Soc.* **1964**, *86*, 5515–5523.
(41) Yeh, A. T.; Shank, C. V.; McCusker, J. K. *Science* **2000**, *289*, 935–938.

(42) McKay, T. J.; Staromlynska, J.; Davy, T. R.; Bolger, J. A. *J. Opt. Soc. Am. B-Opt. Phys.* **2001**, *18*, 358–362.

(43) Staromlynska, J.; McKay, T. J.; Bolger, J. A.; Davy, J. R. *J. Opt. Soc. Am. B-Opt. Phys.* **1998**, *15*, 1731–1736.

(44) Vestberg, R.; Westlund, R.; Eriksson, A.; Lopes, C.; Carlsson, M.; Eliasson, B.; Glimsdal, E.; Lindgren, M.; Malmstrom, E. *Macromolecules* **2006**, *39*, 2238–2246.

(45) McKay, T. J.; Staromlynska, J.; Wilson, P.; Davy, J. *J. Appl. Phys.* **1999**, *85*, 1337–1341.

(46) McKay, T. J.; Bolger, J. A.; Staromlynska, J.; Davy, J. R. *J. Chem. Phys.* **1998**, *108*, 5537–5541.

(47) Dvornikov, A. S.; Rentzepis, P. M. *Opt. Commun.* **1995**, *119*, 341–346.

(48) Parthenopoulos, D. A.; Rentzepis, P. M. *Science* **1989**, *245*, 843–845.

(49) Ehrlich, J. E.; Wu, X. L.; Lee, I. Y. S.; Hu, Z. Y.; Rockel, H.; Marder, S. R.; Perry, J. W. *Opt. Lett.* **1997**, *22*, 1843–1845.

(50) He, G. S.; Xu, G. C.; Prasad, P. N.; Reinhardt, B. A.; Bhatt, J. C.; Dillard, A. G. *Opt. Lett.* **1995**, *20*, 435–437.

(51) Zhao, C. F.; He, G. S.; Bhawalkar, J. D.; Park, C. K.; Prasad, P. N. *Chem. Mater.* **1995**, *7*, 1979–1983.

(52) Denk, W.; Strickler, J. H.; Webb, W. W. *Science* **1990**, *248*, 73–76.

(53) Balaz, M.; Collins, H. A.; Dahlstedt, E.; Anderson, H. L. *Org. Biomol. Chem.* **2009**, *7*, 874–888.

(54) Kawata, S.; Sun, H. B.; Tanaka, T.; Takada, K. *Nature* **2001**, *412*, 697–698.

(55) Yanez, C. O.; Andrade, C. D.; Yao, S.; Luchita, G.; Bondar, M. V.; Belfield, K. D. *ACS Appl. Mater. Interfaces* **2009**, *1*, 2219–2229.

(56) Billone, P. S.; Park, J. M.; Blackwell, J. M.; Bristol, R.; Scaiano, J. C. *Chem. Mater.* **2010**, *22*, 15–17.

(57) Kim, K.-Y.; Shelton, A. H.; Drobizhev, M.; Makarov, N.; Rebane, A.; Schanze, K. S. *J. Phys. Chem. A*, DOI: 10.1021/jp1005567.

(58) The CS state energies are estimated from the relationship, $E_{CS} = E_{1/2}(D/D^+) - E_{1/2}(A/A^-)$, where D is the donor and A is the acceptor. Here we neglect the Coulombic stabilization energy, which would have the effect of raising the energy of the CS states by an amount of ca. 0.1−0.2 eV (depending on the D−A separation distance). We have chosen to neglect this term as it will not affect the relative state orderings, or the major conclusions regarding mechanism discussed below.

(59) Cooper, T. M.; Krein, D. M.; Burke, A. R.; McLean, D. G.; Rogers, J. E.; Slagle, J. E. *J. Phys. Chem. A* **2006**, *110*, 13370–13378.

(60) Cardolaccia, T. *From Molecular Oligomers to Supramolecular Gels: Photophysics of Conjugated Metal-Organic Systems*. Ph.D. Dissertation, University of Florida, Gainesville, FL, 2005; http://www.chem.ufl.edu/~kschanze/index_files/Publications.htm.

JP103531Y